Structural Engineering and Mechanics, *Vol. 65, No. 4 (2018) 359-368*
DOI: https://doi.org/10.12989/sem.2018.65.4.359

Substructure/fluid subdomain coupling method for large vibroacoustic problems

Rabii El Maani[*1,2], Abdelkhalak El Hami[1a] and Bouchaib Radi[2b]

[1]*LMN, INSA de Rouen, Avenue de l'Université, 76800 Saint Etienne de Rouvray, France*
[2]*LIMII, FST Settat, route de Casablanca, Settat, Maroc*

(Received January 6, 2017, Revised December 8, 2017, Accepted January 4, 2018)

Abstract. Dynamic analysis of complex and large structures may be costly from a numerical point of view. For coupled vibroacoustic finite element models, the importance of reducing the size becomes obvious because the fluid degrees of freedom must be added to the structural ones. In this paper, a component mode synthesis method is proposed for large vibroacoustic interaction problems. This method couples fluid subdomains and dynamical substructuring of Craig and Bampton type. The acoustic formulation is written in terms of the velocity potential, which implies several advantages: coupled algebraic systems remain symmetric, and a potential formulation allows a direct extension of Craig and Bampton's method to acoustics. Those properties make the proposed method easy to implement in an existing finite element code because the local numerical treatment of substructures and fluid subdomains is undifferentiated. Test cases are then presented for axisymmetric geometries. Numerical results tend to prove the validity and the efficiency of the proposed method.

Keywords: component mode synthesis; substructure; subdomain; vibroacoustic; finite element; fluid-structure interaction

1. Introduction

The dynamic analysis of complex structures is often expensive and sometimes difficult due to the limitations of computer resources. Moreover, these structures are often composed of several parts that, for organization reasons, are calculated and tested independently of each other by different teams or prepared to make parallel computation (Radi and Estrade 1998).

The substructuring methods are often the only resolution strategy. The use of these methods is therefore justified by numerical computation benefits. One of the most used and effective strategies of dynamic substructuring is based on a modal synthesis technique (modal analysis of each substructure). In Craig (1995), a synthesis of these methods was established. As examples that may be mentioned, those proposed by Craig and Bampton (1968), MacNeal (1971) or Rubin (1975).

Moreover, understanding the mechanisms of interaction between a fluid and an elastic solid is very important in many industrial applications (El Maani *et al*. 2017a, El Maani *et al*. 2017b). When a structure vibrates in the presence of an acoustic fluid, there is interaction between the own airwaves of each region: the fluid flow causes structural deformation and/or the solid deformation causes the fluid movement. These applications require efficient coupling between fluid acoustics and structural dynamics.

In the context of an elastoacoustic study of fluid/structure coupled systems modeled by the finite element method, the interest to reduce the problem's size is obvious because we have to add all the fluid domain degrees of freedom to those of the structure. Then it becomes necessary to reduce the number of unknowns to be treated without losing the accuracy of the solution.

However, the application of a modal synthesis method with a coupled vibroacoustic problem raises two critical issues linked to the choice of the acoustic formulation and the associated method of subdomains.

In fact, without considering the application of substructuring techniques, several finite element formulations have been proposed for the fluid problem when it is coupled to a structure: pressure formulation (Zienkiewicz and Bettess 1978), velocity potential formulation (Everstine 1981), pressure-potential displacement formulation (Morand and Ohayon 1979), velocity pressure-potential formulation (Olson and Bathe 1985), and displacement formulation (Hamdi *et al*. 1978, Olson and Bathe 1983, Wang and Bathe 1997). Each of these methods has its own advantages and disadvantages. A pressure formulation leads to coupled vibroacoustic systems with the classical form $A - \omega^2 B$ (A and B are the stiffness and the mass matrices respectively, assembled for all the fluid and the structure degrees of freedom) but whose matrices are not symmetric, which requires to implement expensive numerical transformations (Iron's transformation) in order to have symmetric systems to solve.

Velocity potential formulations lead to symmetric

∗Corresponding author, Ph.D.
E-mail: rabii.el_maani@insa-rouen.fr
[a]Professor
E-mail: abdelkhalak.elhami@insa-rouen.fr
[b]Professor
E-mail: bouchaib.radi@yahoo.fr

http://www.techno-press.com/journals/sem&subpage=7 ISSN: 1225-4568 (Print), 1598-6217 (Online)

systems, but with a "nonclassical" form $A - \omega^2 B - i\omega C$ (C is the fluid-structure interaction matrix) and require to double the space of resolution to achieve a system that can be used by effective algorithms for searching eigenvalues. Displacement and pressure-potential displacement formulations allow leading directly to symmetrical systems with a classical form, but increasing the number of the degrees of freedom at nodes. Finally, we can mention the special case of displacement formulations discretized by finite element method-based edges (Bermudez *et al*. 1999), extremely interesting numerically, but have a complicated numerical implementation because the degrees of freedom are no longer located at the nodes but on the elements edges.

Regarding the choice of the method of acoustic subdomains, relatively few studies in the literature are proposed contrary to structural dynamics. The explanation is that the acoustic models are generally less expensive numerically (they generally require fewer degrees of freedom per node and the fluid mesh criteria are less restrictive than those of the structures) and therefore do not necessarily need to be reduced (Wang and Bathe 1997, Bennighof 1999). Ait Younes and Hamdi (1997) proposed a subdomains method based on local modes satisfying mixed conditions at the interfaces, and a coupling by Lagrange multipliers (their numerical results, however, concern only the pure acoustics).

Finally, vibroacoustic modal synthesis methods based on pressure formulations for coupling fluid subdomains and substructures have been proposed (Xing *et al*. 1996, Sandberg *et al*. 2001). These methods, in particular, require special processing (making symmetric systems to solve), but quite delicate to implement on an existing calculation code (El Hami and Radi 1996, Radi *et al*. 1994, Sarsri *et al*. 2011).

A technique has been popularized in recent years, this is due to the success that it was encountered in turbulence modelling, it is the Proper Orthogonal Decomposition (POD). It is used in various domains such as aero-acoustics, chemistry, fluid dynamics and more recently in structural mechanics. Its use in the fluid structure interaction domain is under development (Souli and Sigrist 2009).

The aim of this paper is to propose a modal synthesis method for solving large vibroacoustic problems. The developed method couples dynamic substructuring methods of Craig and Bampton type and a method of acoustic subdomains based on an acoustic velocity potential formulation. This choice is guided on one hand by the shape and the symmetry of the obtained coupled algebraic system, and on the other hand by the easy enrichment of the local acoustic modal base. In fact, the choice of a velocity potential formulation allows a direct extension of the Craig and Bampton method to fluid fields. Local modes constitute then modes with perfectly compliant interfaces enriched by incompressible modes of connection (analogy with the static modes of connection in structural dynamics). The results obtained in the case of axisymmetric geometries decomposed into several fluid subdomains and several substructures tend to show the validity and the efficiency of the proposed method.

The paper is organized as follows. In Section 2, we introduce the basic equations of the vibroacoustic problem. In Section 3, we present the variational formulations of the given equations and the finite element discretizations. In Section 4, we give the numerical method to compute the local modes. The modal synthesis is presented in Section 5, and the last section is devoted to a numerical simulation consisting on an elastic ring and a boat propeller.

2. Basic equations

Let be a vibroacoustic problem divided into N_S substructures and N_F fluid subdomains. In the following, exponents (and indices) f and s respectively designate substructures numbers and fluid subdomains. Each substructure and fluid subdomain occupy a volume Ω^s and Ω^f, respectively. There are three kinds of interfaces, defined as follows

$$I^{ss'} = \Omega^s \cap \Omega^{s'},\ J^{ff'} = \Omega^f \cap \Omega^{f'},\ C^{sf} = \Omega^s \cap \Omega^f \tag{1}$$

$I^{ss'}$ denotes the interface between the substructure s and substructure s' ($I^{ss'} = \emptyset$ if these areas are not in contact). $J^{ff'}$ represents the fluid/fluid interface between the fluid subdomains f and f' ($\emptyset$ in the absence of contact). C^{sf} is the fluid/structure interface between the substructure s and the fluid subdomain f ($\emptyset$ if Ω^s and Ω^f are not in contact).

2.1 Equations for structure

We suppose that each substructure is isotropic linear elastic, without initial stress or deformation. In the absence of volume source, the equation that governs their vibrational behaviour is given by

$$\nabla \cdot \sigma^s - \rho_s \ddot{\mathbf{u}}^s = 0, \quad s = 1, \ldots, N_s \tag{2}$$

ρ_s, $\mathbf{u}^s$, σ^s are respectively the density, the displacement field and the stress tensor of the substructure s.

If we denote Γ_u^s the borders of the imposed displacement and Γ_f^s the ones of the imposed external force, the boundary conditions associated with the substructure s are written

$$\mathbf{u}^s\big|_{\Gamma_u^s} = \bar{\mathbf{u}}^s \quad , \quad \sigma^s \cdot n\big|_{\Gamma_f^s} = \bar{f}^s \tag{3}$$

In the substructure/substructure interfaces $I^{ss'}$, continuity of displacement and the normal component of the stress tensor must be ensured. These conditions are written

$$(\mathbf{u}^s - \mathbf{u}^{s'})\big|_{I^{ss'}} = 0 \tag{4}$$

$$(\sigma^s \cdot n - \sigma^{s'} \cdot n)\big|_{I^{ss'}} = 0 \tag{5}$$

2.2 Equations for fluid

We consider small perturbations in adiabatic evolution of a perfect fluid around his rest position. We denote respectively $\mathbf{v}^f$, p^f, ρ_f and c_f, the acoustic velocity, the acoustic pressure, density and the speed of sound of the subdomain *f*. φ^f is the potential of acoustic velocities defined by

$$\mathbf{v}^f = \frac{1}{\rho_f} \nabla \varphi^f \tag{6}$$

Pressure and potential are bound by the following

$$p^f = -\frac{\partial \varphi^f}{\partial t} \tag{7}$$

On the other hand, the velocity potential satisfies the wave equation

$$\frac{1}{\rho_f} \Delta \varphi^f - \frac{1}{\rho_f c_f^2} \ddot{\varphi}^f = 0, \qquad f = 1, \ldots, N_F \tag{8}$$

We denote Γ_φ^s and Γ_v^s, the boundaries with imposed potential (which also means imposing pressure, according to Eq. (7)) and those with imposed normal acoustic velocity. The boundary conditions of the subdomain *f* are

$$\nabla \cdot \sigma^s - \rho_s \ddot{\mathbf{u}}^s = 0, \quad s = 1, \ldots, N_s \tag{9}$$

We note that a treated condition of type wall, with specific acoustic admittance β, imposed on a surface denoted Γ_β^f with normal n (directed to the exterior of the fluid), would be written as $(\partial \varphi^f / \partial n + \beta / c_f \dot{\varphi}^f)\big|_{\Gamma_\beta^f} = 0$. However, we suppose in the following that the structural and the acoustic damping are not assumed.

The continuity conditions to impose on the fluid/fluid interfaces $J^{ff'}$ are based on the continuity of pressure and normal velocity fields

$$(\varphi^f - \varphi^{f'})\big|_{J^{ff'}} = 0 \tag{10}$$

$$\left. \left(\frac{1}{\rho_f} \frac{\partial \varphi^f}{\partial n} - \frac{1}{\rho_{f'}} \frac{\partial \varphi^{f'}}{\partial n} \right) \right|_{J^{ff'}} = 0 \tag{11}$$

2.3 Coupling conditions on fluid-structure interface

If the substructure *s* and the fluid subdomain *f* are in contact, then the coupling conditions in the fluid/structure interface C^{sf} are written

$$\left. \frac{1}{\rho_f} \frac{\partial \varphi^f}{\partial n} \right|_{C^{sf}} = \dot{\mathbf{u}}^s \cdot n \tag{12}$$

$$\sigma^s \cdot n\big|_{C^{sf}} = \dot{\varphi}^f n \tag{13}$$

These conditions correspond respectively to the continuity of the normal velocity and continuity of the normal component of the stress tensor on the interface.

According to the notations above, the borders $\partial\Omega^s$ (resp. $\partial\Omega^f$) of the substructure *s* (resp. subdomain *f*) are completely decomposed in the following manner

$$\begin{aligned} \partial\Omega^s &= \Gamma_u^s \cup \Gamma_f^s \left(\bigcup_{\substack{s'=1 \\ s' \neq s}}^{N_S} I^{ss'} \right) \left(\bigcup_{f=1}^{N_F} C^{sf} \right) \\ \partial\Omega^f &= \Gamma_\varphi^f \cup \Gamma_v^f \left(\bigcup_{\substack{f'=1 \\ f' \neq f}}^{N_F} J^{ff'} \right) \left(\bigcup_{s=1}^{N_S} C^{sf} \right) \end{aligned} \tag{14}$$

3. Variational formulations

3.1 Variational formulation associated with substructures

Let $\mathbf{u}^{s*}$ be a test field associated with the substructure *s*. Eq. (2) is integrated over the area Ω^s. After integration by parts and applying the conditions (3), (5) and (13), the variational problem consists in finding $\mathbf{u}^s$ such as $\left\{ \mathbf{u}^s \big|_{\Gamma_u^s} = \bar{\mathbf{u}}^s \right\}$ and

$$\begin{aligned} &\int_{\Omega^s} \rho_s \mathbf{u}^{s^*} \cdot \ddot{\mathbf{u}}^s dV + \int_{\Omega^s} \varepsilon^{s^*} : \sigma^s dV + \sum_{f=1}^{N_F} \int_{C^{sf}} \mathbf{u}^{s^*} \cdot n \dot{\varphi}^f dS \\ &= \int_{\Gamma_f^s} \mathbf{u}^{s^*} \cdot \bar{f}^s dS + \sum_{\substack{s'=1 \\ s' \neq s}}^{N_s} \int_{I^{ss'}} \mathbf{u}^{s^*} \cdot (\sigma^{s'} \cdot n) dS \\ &\forall \mathbf{u}^{s^*} \Big/ \{ \mathbf{u}^{s^*} \big|_{\Gamma_u^s} = 0 \} \quad s = 1, \ldots, N_s \end{aligned} \tag{15}$$

where ε is the strain tensor and *n* is the outward normal of Ω^s, except on boundaries C^{sf} where it is reentrant (outgoing of Ω^f).

3.2 Variational formulation associated to fluid subdomains

Let φ^{f*} be a test field associated with the subdomain *f*. Eq. (8) is integrated over the area Ω^f. After integration by parts and applying the conditions (9), (11) and (12), the variational problem consists in finding φ^f such as $\left\{ \varphi^f \big|_{\Gamma_\varphi^f} = \bar{\varphi}^f \right\}$ and

$$\begin{aligned} &-\int_{\Omega^f} \frac{1}{\rho_f c_f^2} \varphi^{f^*} \ddot{\varphi}^f dV - \int_{\Omega^f} \frac{1}{\rho_f} \nabla \varphi^{f^*} \cdot \nabla \varphi^f dV + \\ &\sum_{s=1}^{N_S} \int_{C^{sf}} \varphi^{f^*} \dot{\mathbf{u}}^s \cdot n dS = -\int_{\Gamma_v^f} \varphi^{f^*} \bar{v}^f dS - \sum_{\substack{f'=1 \\ f' \neq f}}^{N_F} \int_{J^{ff'}} \varphi^{f^*} \frac{1}{\rho_{f'}} \frac{\partial \varphi^{f'}}{\partial n} dS \\ &\forall \varphi^{f^*} / \{ \varphi^{f^*} \big|_{\Gamma_\varphi^f} = 0 \} \qquad f = 1, \ldots, N_f \end{aligned} \tag{16}$$

where *n* is the outward normal to Ω^f.

3.3 Finite element discretizations

The finite element discretizations of the variational structural (Eq. (15)) and acoustic (Eq. (16)) problems lead to the following algebraic systems

$$\begin{aligned}\langle u^{s^*}\rangle\left([M^s]\{\ddot{u}^s\}+[K^s]\{u^s\}+\sum_{f=1}^{N_F}\left[C^{sf}\right]\{\dot{\varphi}^f\}\right)=\\ \langle u^{s^*}\rangle\left(\{f^s\}+\sum_{\substack{s'=1\\ s'\neq s}}^{N_S}\{f_I^{ss'}\}\right)\qquad s=1,\ldots,N_s\end{aligned}\tag{17}$$

$$\begin{aligned}\langle \varphi^{f^*}\rangle\left(-[Q^f]\{\ddot{\varphi}^f\}-[H^f]\{\varphi^f\}+\sum_{s=1}^{N_S}\left[C^{sf}\right]^T\{\dot{u}^s\}\right)=\\ -\langle \varphi^{f^*}\rangle\left(\{\nu^f\}+\sum_{\substack{f'=1\\ f'\neq f}}^{N_F}\{\nu_J^{ff'}\}\right)\qquad f=1,\ldots,N_F\end{aligned}\tag{18}$$

The correspondences of the different discretized terms with those of the formulations (15) and (16) are shown in their order of appearance. The notations $\langle\cdot\rangle$ and $\{\cdot\}$ designate the row and column vectors, respectively.

$\{u^s\}$ and $\{\varphi^f\}$ contains all the unknown degrees of freedom associated with the structural displacement and the acoustic potential, respectively (the degrees of freedom of the Γ_u^s and Γ_φ^s boundaries, already known, are not contained in these vectors). $[M^s]$, $[K^s]$ and $\{f^s\}$ denote the mass matrix of the substructure s, its rigidity matrix and its external equivalent forces vector. $[Q^f]$, $[H^f]$ and $\{\nu^f\}$ represent the mass matrix of the subdomain f, its stiffness matrix and its external acoustic excitations vector. The terms, ambiguous, of "mass" and the acoustic "rigidity" are respectively associated with the potential and kinetic acoustic energy.

The term $\{f_I^{ss'}\}$ represents physically the interfacial forces on the substructure s by the adjacent substructure s'. Similarly, the term $\{\nu_I^{ff'}\}$ is the interfacial actions exerted on f by the adjacent fluid subdomain f'. Their effects are applied only on the degrees of freedom of the concerned interface.

We assemble the substructures N_S and the acoustic subdomains N_F on a global vector containing all the degrees of freedom, structure and fluid, organized according to the following form

$$\langle u\rangle=\langle u^1\, u^2\ldots u^{N_s}\,|\,\varphi^1\,\varphi^2\ldots\varphi^{N_F}\rangle\tag{19}$$

So, taking into account that we can take any test vector $\langle u^*\rangle$, we can show that the assembly of the formulations (17) and (18) yields the following algebraic system

$$[M]\{\ddot{u}\}+[C]\{\dot{u}\}+[K]\{u\}=\{f\}+\{f_I\}\tag{20}$$

where

$$[M]=\begin{bmatrix}M^1 & & 0 & 0 & & 0\\ & \ddots & & & & \\ 0 & & M^{N_s} & 0 & & 0\\ 0 & & 0 & -Q^1 & & 0\\ & & & & \ddots & \\ 0 & & 0 & 0 & & -Q^{N_F}\end{bmatrix}$$

$$[K]=\begin{bmatrix}K^1 & & 0 & 0 & & 0\\ & \ddots & & & & \\ 0 & & K^{N_s} & 0 & & 0\\ 0 & & 0 & -H^1 & & 0\\ & & & & \ddots & \\ 0 & & 0 & 0 & & -H^{N_F}\end{bmatrix}$$

$$[C]=\begin{bmatrix}0 & & 0 & C^{11} & \ldots & C^{1N_F}\\ & \ddots & & \vdots & & \vdots\\ 0 & & 0 & C^{N_S1} & \ldots & C^{N_SN_F}\\ & & & 0 & & 0\\ & sym & & & \ddots & \\ & & & 0 & & 0\end{bmatrix}$$

$$\{f\}=\begin{Bmatrix}f^1\\ \vdots\\ f^{N_S}\\ -\nu^1\\ \vdots\\ -\nu^{N_F}\end{Bmatrix},\quad \{f_I\}=\begin{Bmatrix}\sum_{s'\neq 1} f_I^{1s'}\\ \vdots\\ \sum_{s'\neq N_S} f_I^{N_Ss'}\\ -\sum_{f'\neq 1}\nu_J^{1f'}\\ \vdots\\ -\sum_{f'\neq N_F}\nu_J^{N_Ff'}\end{Bmatrix}$$

In the above expressions, the matrices $[C^{sf}]$ are implicitly null when there is no interface between Ω^s and Ω^f ($C^{sf}=\emptyset$).

The matrices $[M]$, $[C]$ and $[K]$ are symmetrical. This characteristic is essential since it allows achieving coupled eigenmodes that satisfy orthogonality properties. The last term in Eq. (20) will disappear later when it will be forced by the continuity of displacements between the substructures and the continuity of pressures between the fluid subdomains.

For large size vibroacoustic problems, the resolution of the assembled global system (20) can become very costly in terms of memory and computation time.

4. Computation of local modes

4.1 Local modes of substructures

The vector of degrees of freedom of each substructure s is partitioned according to internal degrees of freedom (subscript i) and those with junctions (index j). The latter correspond to the degrees of freedom positioned at the interfaces between the substructure s and all other adjacent substructures. This becomes

$$\langle u^s\rangle=\langle u_i^s\; u_j^s\rangle,\ [M^s]=\begin{bmatrix}M_{ii}^s & M_{ij}^s\\ M_{ji}^s & M_{jj}^s\end{bmatrix},\ [K^s]=\begin{bmatrix}K_{ii}^s & K_{ij}^s\\ K_{ji}^s & K_{jj}^s\end{bmatrix}\tag{21}$$

Following the Craig and Bampton method, the selected local modes correspond to modes with fixed interfaces $I^{ss'}$. They check the problem with the following eigenvalues systems

$$[K_{ii}^s - \omega^2 M_{ii}^s]\{\psi_i^s\} = 0, \qquad s = 1,\ldots,N_S \tag{22}$$

These orthogonal modes are enriched by static binding modes, which are defined as the static deformation of the considered substructure when a unit displacement is applied alternately to each of its degrees of freedom of junction; the others are forced to be set to 0.

Local modal basis of a substructure is thus given by

$$[\Psi^s] = \begin{bmatrix} \psi^s & -K_{ii}^{s-1}K_{ij}^s \\ 0 & I_{jj}^s \end{bmatrix} \tag{23}$$

where $[\Psi^s]$ represents the modes matrix with fixed interfaces arranged in columns.

The physical degrees of freedom of each substructure may then be decomposed to their respective local modal base

$$\{u^s\} = [\Psi^s]\{\alpha^s\}, \qquad s = 1,\ldots,N_S \tag{24}$$

$\{\alpha^s\}$ is the vector of generalized coordinates associated with the substructure *s*, containing on one hand the coefficients associated with the fixed interfaces modes, and on the other hand the physical degrees of freedom (nodal displacements, rotations,...) with structural junction.

4.2 Local modes of acoustic subdomains

The form of the fluid algebraic system, inherent for the velocity potential formulation, allows a direct extension of the Craig and Bampton method. Performing a similar partitioning to what was described for the substructures, we write

$$\langle\varphi^f\rangle = \langle\varphi_i^f \;\; \varphi_j^f\rangle,\; [Q^f] = \begin{bmatrix} Q_{ii}^f & Q_{ij}^f \\ Q_{ji}^f & Q_{jj}^f \end{bmatrix},\; [H^f] = \begin{bmatrix} H_{ii}^f & H_{ij}^f \\ H_{ji}^f & H_{jj}^f \end{bmatrix} \tag{25}$$

We define local modes with perfectly compliant interfaces $J^{ff'}$ (zero pressure) by

$$[H_{ii}^f - \omega^2 Q_{ii}^f]\{\phi_i^f\} = 0, \qquad f = 1,\ldots,N_F \tag{26}$$

The enrichment of this base is obtained by direct analogy with the static modes of connection in structural dynamics. For the acoustic, these modes correspond physically to incompressible modes of connection ($C_f \to \infty$ is equivalent $\omega \to 0$). They are defined as the incompressible response of the considered subdomain, when a potential unit is applied alternately to each of its degrees of freedom with a fluid junction, the others being forced to 0. Finally, the local modal base of a fluid subdomain *f* is given by

$$[\Phi^f] = \begin{bmatrix} \phi^f & -H_{ii}^{f-1}H_{ij}^f \\ 0 & I_{jj}^f \end{bmatrix} \tag{27}$$

where $[\phi^f]$ represents the matrix of modes with compliant interfaces arranged in columns.

The physical degrees of freedom of each fluid subdomain may then be decomposed to their respective local modal base

$$\{\varphi^f\} = [\Phi^f]\{\beta^f\}, \qquad f = 1,\ldots,N_F \tag{28}$$

$\{\beta^f\}$ is the vector of generalized coordinates associated with the subdomain *f*, containing the coefficients associated with modes of compliant interfaces, and also the physical degrees of freedom (i.e. nodal potentials) of fluid junction.

Finally, it should be noted that a direct extension of the Craig and Bampton method to acoustics appears feasible for pressure formulations or potential formulations. The shape of the other types of acoustic formulations prevents a priori to consider the static case (ω = 0) or the incompressible case for establishing the enrichment modes.

5. Modal synthesis

5.1 Model reduction

Local decompositions (24) and (28) can be assembled as follows

$$\{u\} = [\Psi]\{p\} \tag{29}$$

with

$$[\Psi] = \begin{bmatrix} \Psi^1 & 0 & 0 & 0 \\ & \ddots & & \\ 0 & \Psi^{N_s} & 0 & 0 \\ 0 & 0 & \Phi^1 & 0 \\ & & & \ddots \\ 0 & 0 & 0 & \Phi^{N_F} \end{bmatrix},\; \{p\} = \begin{Bmatrix} \alpha^1 \\ \vdots \\ \alpha^{N_s} \\ \beta^1 \\ \vdots \\ \beta^{N_F} \end{Bmatrix} \tag{30}$$

Then, Eq. (20) becomes after projection of Eq. (29)

$$[M_p]\{\ddot{p}\} + [C_p]\{\dot{p}\} + [K_p]\{p\} = \{f_p\} + [\Psi]^T\{f_I\} \tag{31}$$

with

$$\begin{gathered} [M_p] = [\Psi]^T[M][\Psi],\;\; [C_p] = [\Psi]^T[C][\Psi] \\ [K_p] = [\Psi]^T[K][\Psi],\;\; \{f_p\} = [\Psi]^T\{f\} \end{gathered} \tag{32}$$

We must now consider the continuity conditions at the interfaces structure/structure and fluid/fluid. Indeed, the degrees of freedom of $\{p\}$ are not linearly independent. The linear relation between the degrees of freedom is issues from equal displacement at the structure/structure interfaces and equal pressure at the fluid/fluid interfaces. They can be expressed by a connectivity global matrix $[S]$

$$\{p\} = [S]\{q\} \tag{33}$$

where $\{q\}$ contains only linearly independent degrees of freedom. $[S]$ characterizes both the connectivity between the substructures and the connectivity between the fluid subdomains. For the Craig and Bampton type of method as it is the case here, the matrix $[S]$ is Boolean and easy to express because the junction physical degrees of freedom are explicitly a part of the generalized unknown $\{p\}$.

Then, Eq. (31) becomes

$$\left[M_q\right]\{\ddot{q}\}+\left[C_q\right]\{\dot{q}\}+\left[K_q\right]\{q\}=\left\{f_q\right\}+\left[S\right]^T\left[\Psi\right]^T\left\{f_I\right\} \quad (34)$$

with

$$\begin{gathered}[M_q]=[S]^T[M_p][S],\ [C_q]=[S]^T[C_p][S]\\ [K_q]=[S]^T[K_p][S],\ \{f_q\}=[S]^T\{f_p\}\end{gathered} \quad (35)$$

According to the conditions (5) and (11), the mutually reactive interface forces (i.e., not including external forces applied at the interface) are related by

$$\left\{f_I^{ss'}\right\}+\left\{f_I^{s's}\right\}=0, \qquad \left\{\nu_J^{ff'}\right\}+\left\{\nu_J^{f'f}\right\}=0 \quad (36)$$

We can then show that these equations with the displacement compatibility equation involve $\left[S\right]^T\left[\Psi\right]^T\left\{f_I\right\}=0$, (for details, see (Craig 1995)).

Thus, the final system to be solved is

$$\left[M_q\right]\{\ddot{q}\}+\left[C_q\right]\{\dot{q}\}+\left[K_q\right]\{q\}=\left\{f_q\right\} \quad (37)$$

Compared to the system (20), this model is significantly reduced in practice since its size corresponds to the total number of orthogonal local modes retained after truncation, which must be added to the total number of junction's degrees of freedom.

5.2 Computation of coupled eigenmodes

To enable the use of effective algorithms for searching eigenvalues, the system must first be set in the following equivalent form

$$[A]\{y\}+[B]\{\dot{y}\}=\{F\} \quad (38)$$

where

$$\{y\}=\begin{Bmatrix}q\\ \dot{q}\end{Bmatrix},\ [A]=\begin{bmatrix}K_q & 0\\ 0 & -M_q\end{bmatrix},\ [B]=\begin{bmatrix}C_q & M_q\\ M_q & 0\end{bmatrix},\ \{F\}=\begin{Bmatrix}f_q\\ 0\end{Bmatrix} \quad (39)$$

The resolution space is thus artificially doubled. The two matrices $[A]$ and $[B]$ are real and symmetric.

We set a time dependence of the form $\{y\}=\{y_m\}e^{-i\omega_m t}$. The global modes of the coupled fluid structure system are then obtained by solving the problem with the following global eigenvalues

$$\left([A]-i\omega_m[B]\right)\left\{y_m\right\}=\left\{0\right\} \quad (40)$$

The resolution of this problem leads to pairs of eigenpulsations with opposite real parts associated with complex conjugated eigenvectors. The properties of orthogonality are preserved because of the matrices symmetry. If we choose normalization relative to the mass matrix of the coupled system, given by $\langle\bar{q}_n\rangle[M_q]\{q_n\}=1$, then we show that these properties are written

$$\langle\bar{y}_n\rangle\left[B\right]\left\{y_m\right\}=a_m\delta_{nm}, \quad \langle\bar{y}_n\rangle\left[A\right]\left\{y_m\right\}=i\omega_m a_m\delta_{nm} \quad (41)$$

where $a_m=\langle\bar{q}_m\rangle\left[C_q\right]\left\{q_m\right\}+2\mathrm{Im}(\omega_m)$ and δ_{nm} denotes the Kroenecker symbol and the bar represents the conjugated (complex). Note that the imaginary parts of pulsations are zero because we have neglected any damping.

In case where a structural or acoustic damping would be taken into account, the described method and the resolution techniques remain unchanged: the matrix $[C]$ corresponds to a matrix including both the coupling and the damping effects. The only difference will be the eigenpulsations obtained at nonzero imaginary parts.

5.3 Computation of the vibroacoustic response

The desired vibroacoustic response is now decomposed on the coupled modal basis obtained previously

$$\{y\}=\left[Y\right]\{\alpha\} \quad (42)$$

where the matrix $[Y]$ corresponds to the modes matrix $\{y_m\}$ arranged in column (m = 1,…,M where M is the number of coupled modes retained after truncation). The orthogonality properties (41) are then used to diagonalize the system (38), by posing $h_m=a_m^{-1}\langle\bar{y}_m\rangle\{F\}$ we have

$$\dot{\alpha}_m+i\omega_m\alpha_m=h_m \quad (43)$$

The solution of this equation is given analytically by

$$\alpha_m(t)=\int_0^t e^{-i\omega_m(1-\tau)}h_m(\tau)d\tau+\alpha_m(0)e^{-i\omega_m t} \quad (44)$$

We can perform a Fourier transformation of Eq. (43), resulting in the following frequency response

$$\alpha_m(\omega)=\frac{h_m(\omega)}{i(\omega_m-\omega)} \quad (45)$$

The physical response is then reconstituted by the successive transformations (43), (33) and (29).

Table 1 Geometrical and physical parameters

Structure parameters	Young's Mod. E (GPa)	Density μ (Kg/m^3)	h (m)	R (m)
	210	7800	0.05	0.5
Fluid parameters	-	Density ρ (Kg/m^3)	R' (m)	R (m)
	-	1000	0.3	0.5

6. Numerical simulation

In order to demonstrate the efficiency of this method, two fluid structure interaction applications are treated below, the first is a two-dimensional circular elastic ring in which we validate separately the inertial effect of the fluid, the acoustic subdomains method, the substructuring method and then the coupled substructures with the acoustic fluid. The second application is a two-dimensional boat propeller decomposed into 4 substructures and coupled with fluid domain, results of the dry and the submerged model are then presented. These applications show the possibility to use a parallel computer to make the computation (Radi and Estrade 1998).

6.1 Elastic ring

6.1.1 Problem statement

The aim being to validate the proposed method, a two-dimensional model is created, with axisymmetric geometry. A structural ring is coupled to a closed fluid volume that is filled with water to simulate the strong coupling between

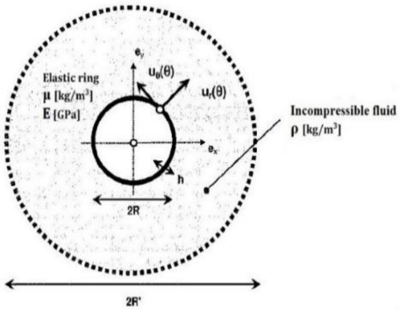

Fig. 1 Elastic ring coupled with an incompressible fluid contained in a cylindrical cavity

the structure and the fluid. It is about to calculate the modes of flexion and traction of an elastic ring of radius R, thickness h, density μ and Young's modulus E, contained in a circular cavity of radius R' and containing a fluid with density ρ. The finite element system matrices are generated in the commercial program ANSYS using the implemented fluid-structure coupling scheme (Kim *et al*. 2014, Bendaou *et al*. 2009). The finite element model consists of quadrilateral structural and fluid elements, namely FLUID29 and PLANE42 elements in ANSYS. The interface lines contain both the fluid and the structural degrees of freedom; the bold line represents the structural ring as illustrated in Fig. 1.

6.1.2 Modal anlysis

The geometrical and physical parameters of the treated problem are presented in Table 1. Modal calculations are made with I = 192 fluid finite element.

Table 2 Characterization of the inertial effect

Fourier Component	β
m = 0	-
m = 1	-
m = 2	67.5%
m = 3	69.8%
m = 4	73/1%
m = 5	75.4%

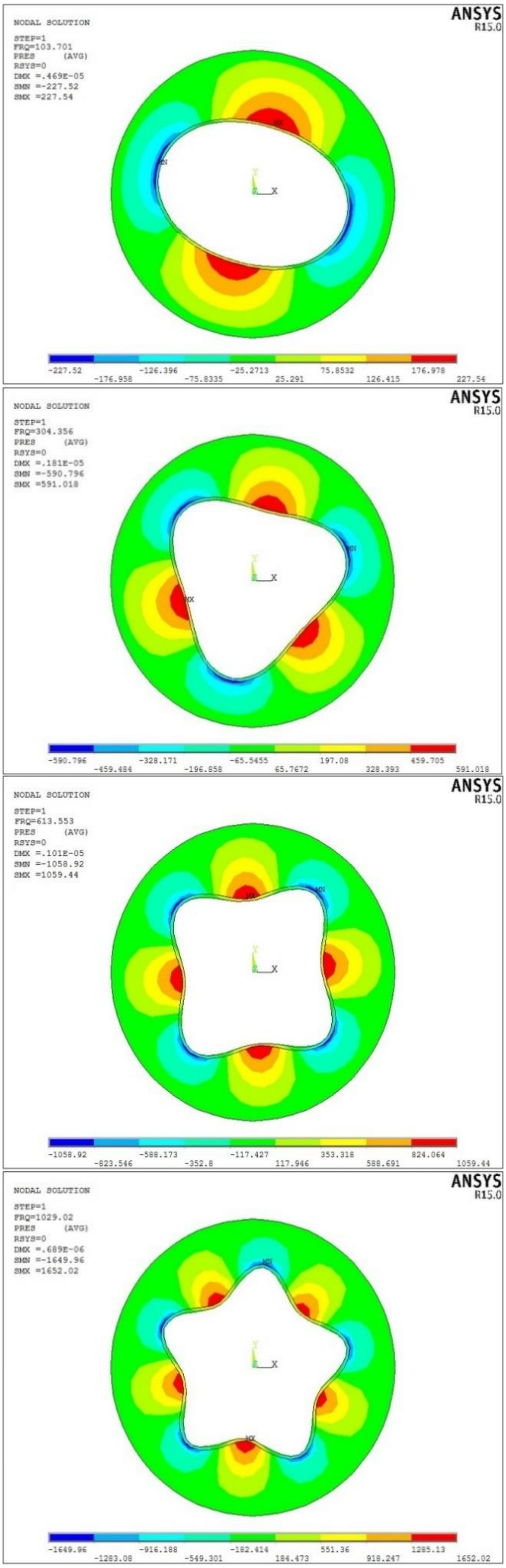

Fig. 2 Mode shapes of the elastic ring coupled with an incompressible fluid, Fourier component m = 2 to m = 5

Table 3 Analytical and numerical computation of eigenfrequencies for submerged elastic ring

Eigenfrequencies (Hz)	Analytical solution	Numerical computation
F_3	104	103.70
F_4	307	304.36
F_5	607	613.55
F_6	1004	1029.0

Table 2 characterizes the inertial effect using the coefficient $\beta = f_{with\ fluid} / f_{without\ fluid}$, ratio of the eigenfrequencies of the modes with and without fluid for each Fourier component

m = 0 to m = 5. For the components m = 0 and m = 1, the eigenmodes correspond respectively to the rotation and translation of the ring; these are modes of rigid body which does not generate fluid movement.

The inertial effect is less marked for higher-order modes. This is highlighted in a quantitative manner by calculating the added mass and qualitative manner with the appearance of the pressure field, whose fluctuations are more localized around the ring. The higher order modes generate local movements of the fluid: the associated kinetic energy is lower than for global movements, which leads to a smaller inertial effect.

Table 3 provides, for the Fourier components m=2 to m=5, a comparison of numerical and analytical calculations of the eigenfrequencies of the submerged elastic ring to which we superpose the field pressure of the fluid, derived from the relation (Sigrist 2011): $P_m = -\rho\omega^2 K_F^{-1} R^T U_m$, and Fig. 2 provides a representation of the ring mode shapes.

The next section aims to show the accuracy and efficiency of the presented method. Figs. 3-4 show the substructures and subdomains partitions that are composed by the presented FSI substructure technique.

6.1.3 Acoustic circular cavity decomposed into subdomains

This first test case is intended only to validate the subdomains method for acoustics, without coupling. It concerns a circular cavity of fluid, splitted into two and four subdomains (see Figs. 3(b)-(c)). The walls of the cavity are perfectly rigid. Table 4 indicates the eigenfrequencies of the cavity obtained for the full model and according to subdomains techniques.

The results are in good agreement, and the relative errors $\Delta f_{\text{rel}} = (f_{(b,c)} - f_{(a)}) / f_{(a)}$, with respect to the reference frequency $f_{(a)}$ from the full model, are displayed and they are satisfactory and do not exceed 0.2%. The proposed method can treat a big size problem and it is very good adapted to parallel computer.

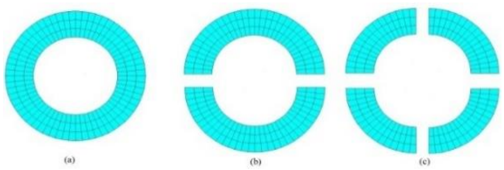

Fig. 3 Finite element mesh of subdomains

Table 4 Eigenfrequencies of the circular cavity with rigid walls

Eigenfrequencies (Hz)	Full model (a)	Subdom. (b)	Subdom. (c)
1	-	-	-
2	603.36	603.36 (0.0%)	603.39 (0.0%)
3	1204.4	1204.4 (0.0%)	1204.4 (0.0%)
4	1801.1	1801.1 (0.0%)	1802.0 (0.04%)
5	2391.5	2391.5 (0.0%)	2391.5 (0.0%)
6	2974.7	2974.7 (0.0%)	2979.1 (0.14%)

6.1.4 Elastic ring decomposed into substructures

Table 5 gives the eigenfrequencies of the dry structure (without coupling with the surrounding fluid). The ring is also splitted into two and four substructures of equal length which means two interfaces for each substructure (Fig. 4).

Table 6 gives the coupled eigenfrequencies reconstituted of the fluid/structure system (Fig. 5). The resolution requires this time to double the resolution space, as indicated in section 6. The results show the validity of the method, since the error remains below 0.2%.

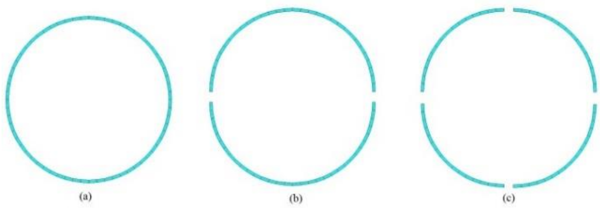

Fig. 4 Finite element mesh of substructures

Table 5 Eigenfrequencies of the dry elastic ring

Eigenfrequencies (Hz)	Full model (a)	Substr. (b)	Substr. (c)
F_3	153.51	153.51 (0.0%)	153.51 (0.0%)
F_4	435.47	435.51 (0.01%)	435.47 (0.0%)
F_5	838.54	838.61 (0.01%)	838.54 (0.0%)
F_6	1363.6	1364.3 (0.05%)	1363.7 (0.01%)

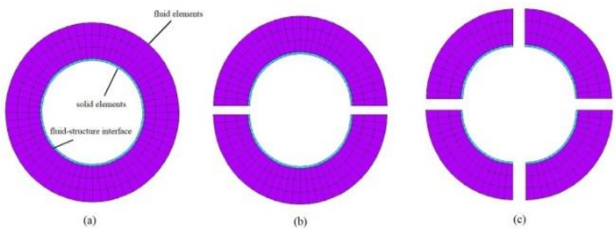

Fig. 5 Finite element mesh of the submerged ring

Table 6 Eigenfrequencies of the submerged ring

Eigenfrequencies (Hz)	Full model (a)	Substr. (b)	Substr. (c)
F_3	103.70	103.70 (0.0%)	103.70 (0.0%)
F_4	304.36	304.25 (0.0%)	303.71 (0.2%)
F_5	613.55	612.04 (0.2%)	613.73 (0.03%)
F_6	1029.0	1038.2 (0.9%)	1021.7 (0.7%)

Table 6 gives the eigenfrequencies of the dry structure (obtained by direct numerical computation). We can clearly see the effect of coupling, which is manifested in eigenfrequencies decrease. The adequacy of the results obtained by direct calculation and substructures tends to prove the validity and effectiveness of the proposed vibroacoustic substructuring method, because we don't lose any information about the computed frequencies.

6.2 Boat propeller

We study the dynamic behavior of a boat propeller. The geometrical model of this propeller (Fig. 6) was designed by means of “ANSYS”. The mesh as well as the geometrical substructuring (Fig. 7) was carried out with “ANSYS”.

The mesh was made with quadrilateral elements. For calculation with modal synthesis (dofs reduction), we divide the propeller into four substructures, and we present the found results for the full model and the four substructures taking into account fluid structure interaction.

The material properties of the treated problem are presented in Table 7.

In Tables 8-9, the modal analysis of the boat propeller is presented and the computed eigenfrequencies are compared.

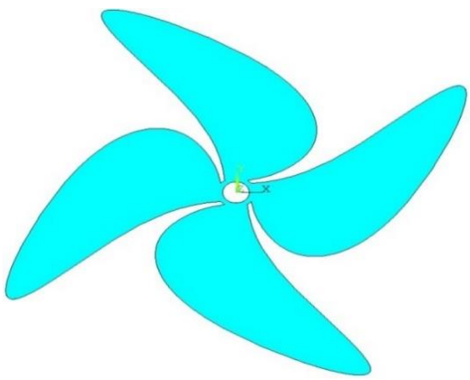

Fig. 6 Boat propeller

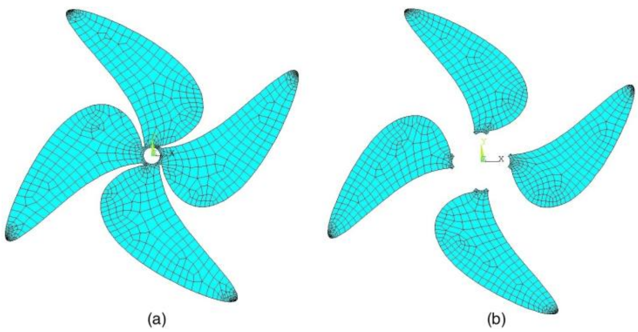

Fig. 7 Finite element mesh and substructuring

Table 7 Material properties

Structure parameters	Young’s Mod. E (GPa)	Density ρ_s (Kg/m^3)	Poisson ratio v
	96	9200	0.3
Fluid parameters	Sound speed c (m/s)	Density ρ_f (Kg/m^3)	-
	1500	1000	-

Table 8 Experimental and numerical modal analysis of the boat propeller

Eigenfrequencies (Hz)			
Dry propeller		Submerged propeller	
Experimental results	Numerical results	Experimental results	Numerical results
73	68.96	36	36.76
117	111.05	65	64.91
201	188.32	123	120.22

Table 9 Eigenfrequencies of the boat propeller

Submerged propeller	
Full model (a)	Substr. (b)
36.76	35.47 (0.01%)
64.91	64.02 (0.0%)
120.22	122.91 (0.02%)

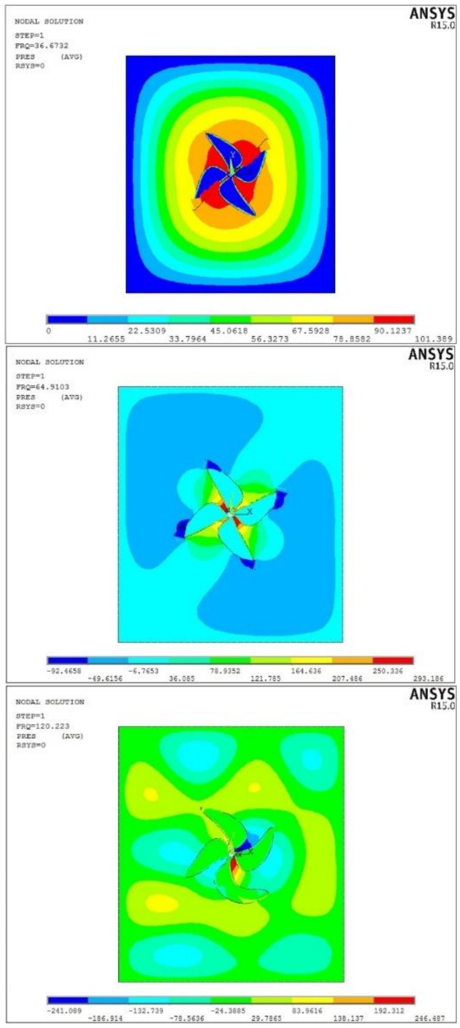

Fig. 8 Eigenmodes of the substructure components

First, we compare our numerical results with the experimental ones (Devic *et al*. 2005) in both dry and submerged cases and then we give the found results for the substructure components of the submerged propeller. The eigenmodes are exposed in Fig. 8.

7. Conclusions

In this paper, we propose a modal synthesis method to solve the coupled fluid-structure problems of large size. The developed method couples dynamic substructuring method of Craig and Bampton type and a method of acoustic subdomains based on an acoustic formulation in velocity potential. This choice implies several advantages. First, the coupled algebraic system remains symmetrical so the modes always satisfy the orthogonality properties. Then the formulation allows a direct extension of the Craig and Bampton method to acoustics. However, the eigenvalue problem resolution by conventional algorithms requires doubling the space resolution.

The obtained results in the case of axisymmetric geometries tend to show the validity and the potential of the proposed method, which has several interests. First, it is relatively easy to implement in existing codes of calculation since the local treatment of substructures and fluid subdomains is undifferentiated. Then, the global matrix of the fluid-structure coupling is susceptible to include directly the damping effects (structural and acoustic) without any notable modification in the method. The proposed method allows making only a single synthesis, without an intermediate synthesis of uncoupled acoustic and structural global modes (for a formulation under pressure, this intermediate synthesis should generally be performed to symmetrize the coupled system). Finally, the FE computation can be done in parallel computer.

Acknowledgments

The authors would like to thank “PHC Volubilis MA/13/292: Integrated action Morocco France” for their financial support for the realization of this work.

References

Ait Younes, T. and Hamdi, M.A. (1997), *Computational Acoustics and Its Environmental Applications II, Modal Shapes Reconstruction Method for Large Domains (Structure and Acoustic)*, Computational Mechanics Publications, 129-137.

Bendaou, O., Rojas, J.E., El Hami, A., Annaque, A. and Agouzoul, M. (2009), “Stochastique and reliability analysis of a propeller with model reduction”, *Eur. J. Comput. Mech.*, **18**(2), 153-173.

Bennighof, J. (1999), “Vibroacoustic frequency sweep analysis using automated multi-level substructuring”, *AIAA J.*, **1**, 422-427.

Bermudez, A., Hervella-Nieto, L. and Rodriguez, R. (1999), “Finite element computation of three-dimensional elastoacoustic vibrations”, *J. Sound Vibr.*, **219**, 279-306.

Corigliano, A., Dossi, M. and Mariani, S. (2013), “Domain decomposition and model order reduction methods applied to the simulation of multi-physics problems in MEMS”, *Comput. Struct.*, **122**, 113-127.

Craig, R.R. (1995), “Substructure methods in vibration”, *J. Vibr. Acoust.*, **117**, 207-213.

Craig, R.R. and Bampton, M.C. (1968), “Coupling of substructures for dynamic analyses”, *A.I.A.A. J.*, **6**, 1313-1319.

Devic, C., Sigrist, J.F., Lain, C. and Baneat, P. (2005), “Etude modale numérique et expérimentale d’une hélice marine”, *Proceedings of Septième Colloque National en Calcul des Structures*, **1**, 277-282.

El Hami, A. and Radi, B. (1996), “Some decomposition methods in the analysis of repetitive structures”, *Comput. Struct.*, **58**(5), 973-980.

El Maani, R., Makhloufi, A., Radi, B. and El Hami, A. (2017a), RBDO analysis of the aircraft wing based aerodynamic behavior, *Struct. Eng. Mech.*, **61**, 441-451.

El Maani, R. Radi, B. and El Hami, A. (2017b), “Vibratory reliability analysis of an aircraft’s wing via fluid-structure interactions”, *J. Aerosp.*, **4**(3), 40.

Everstine, G.C. (1981), “A symmetric potential formulation for fluid-structure interaction”, *J. Sound Vibr.*, **79**, 157-160.

Hamdi, M.A. and Ousset, Y. and Verchery, G. (1978), “A displacement method for the analysis of vibrations of coupled fluid-structure systems”, *J. Numer. Meth. Eng.*, **13**, 139-150.

Kim, S., Choi, E., Lee, S. and Lim, O. (2014), “Semi-analytical numerical approach for the structural dynamic response analysis of spar floating substructure for offshore wind turbine”, *Struct. Eng. Mech.*, **52**(3), 633-646.

MacNeal, R.H. (1971), “Domain decomposition and model order reduction methods applied to the simulation of multi-physics problems in MEMS”, *Comput. Struct.*, **1**, 581-601.

Morand, H. and Ohayon, R. (1979), “Substructure variational analysis of the vibration of coupled fluid-structure systems. Finite element results”, *J. Numer. Meth. Eng.*, 741-755.

Olson, L.G. and Bathe, K.J. (1983), “A study of displacement-based fluid finite elements for calculating frequencies of fluid and fluid-structure systems”, *Nucl. Eng. Des.*, **76**, 137-151.

Olson, L.G. and Bathe, K.J. (1985), “Analysis of fluid-structure interactions. A direct symmetric coupled formulation based on the fluid velocity potential”, *Comput. Struct.*, **21**, 21-32.

Radi, B. and Estrade, J.F. (1998), “Adaptive parallelization techniques in global weather models”, *Parall. Comput.*, **24**, 1167-1175.

Radi, B., Gelin, C. and Perriot, A. (1994), “Subdomain methods in structural mechanics”, *J. Numer. Meth. Eng.*, **37**, 3309-3322.

Rubin, S. (1975), “Improved component-mode representation for structural dynamic analysis”, *A.I.A.A. J.*, **13**, 995-1006.

Sandberg, G.E., Hansson, P.A. and Gustavsson, M. (2001), “Domain decomposition in acoustic and structure-acoustic analysis”, *Comput. Meth. Appl. Mech. Eng.*, **190**, 2979-2988.

Sarsri, D., Azrar, L., Jebbouri, A. and El Hami, A. (2011), “Component mode synthesis and polynomial chaos expansions for stochastic frequency functions of large linear FE models”, *Comput. Struct.*, **89**, 346-356.

Sigrist, J.F. (2011), *Interaction Fluide-Structure, Analyse Vibratoire Par Eléments Finis*, Ellipse, Paris, France.

Souli, M. and Sigrist, J.F. (2009), *Interaction Fluide-Structure: Modélisation et Simulation Numérique*, Hermès, Paris, France.

Wang, X. and Bathe, K.J. (1997), “Displacement/pressure based mixed finite element formulations for acoustic fluid-structure interaction problems”, *J. Numer. Meth. Eng.*, **40**, 2001-2017.

Xing, J.T., Price, W.G. and Du, Q.H. (1996), “Mixed finite element substructure-subdomain methods for the dynamical analysis of coupled fluid-solid interaction problems”, *Philosoph. Trans. Roy. Soc. Lond. Ser. A Math. Phys. Eng. Sci.*, **354**, 259-295.

Zienkiewicz, O.C. and Bettess, P. (1978), “Fluid-structure dynamic interaction and wave forces. An introduction to numerical treatment”, *J. Numer. Meth. Eng.*, **13**, 1-16.

PL